Int. j. adv. multidisc. res. stud. 2023; 3(6):1560-1566

Received: 10-11-2023
Accepted: 20-12-2023

International Journal of Advanced Multidisciplinary Research and Studies

ISSN: 2583-049X

Impact on Seismic Risk Analysis of Possible Pulse in Nearby Areas

[1] Mohammad Sadigh Sarabi, [2] Seyyed Arash Sohrabi, [3] Samad Dehghan, [4] Nima Gheitarani

[1] Department of Civil Engineering, Islamic Azad University of Marand, Iran
[2, 3] Department of Education, Construction Engineering Organization of East Azarbaijan Province, Iran
[4] Arizona State University, School of Sustainability, Tempe, A.Z., United States

DOI: https://doi.org/10.62225/2583049X.2023.3.6.3285
Corresponding Author: **Mohammad Sadigh Sarabi**

Abstract

Seismic risk analysis is the basis of advanced seismic regulations of the world. Therefore, extensive research is being done in the field of seismic risk analysis to solve the previous weaknesses of seismic risk analysis. Classical probabilistic seismic risk analysis (Cornell's method) estimates the seismicity of the region by considering the uniform distribution over the area and the large area. This characteristic causes the seismicity of the area is not estimated correctly in the areas near the fault, because the movement of the earth in this area is different from the far area. In this research, the effect of pulse on the results of probabilistic risk analysis has been investigated. The obtained results indicate that the pulse effects have a significant effect on the acceleration spectrum at close distances within the period limit of 0.2 to 1. So in the period of 0.5, this difference reaches 50% and with the increase of the distance the impact of the pulse decreases in the period limit and the amount of increase in the range of the spectrum decreases.

Keywords: Earthquake, Probability Pulse and Cornell Method, Seismic Hazard

1. Introduction

Engineering structures must be designed in such a way that they can withstand earthquakes without any damage or little damage, therefore, the design of such structures requires an accurate estimation of the risk of the area, and it is very necessary to consider the important features of seismic risk. Seismic risk analysis is used to quantitatively assess the seismic risk of an area and determine the quantity of these earthquakes in the regulations (Farrokhirad & Gheitarani, 2024) [6]. Seismic risk analysis is done in two ways: Deterministic Seismic Risk Analysis (DSHA) and Probabilistic Seismic Risk Analysis (PSHA), (Naghibi Iravani *et al*., 2024b) [23]. In selecting the design earthquake and also calculating its value, when a structure is located near the fault, it is very important due to the existence of special characteristics of the earthquake in the nearby area, and special attention should be paid to this issue (Norouzian & Sarabi 2023) [20].

In the conditions of the near field, the response of the structure and ground motion is especially different from the far field. Such earthquake waves can cause serious damage to modern malleable buildings (Karimimansoob *et al*., 2024-a) [14]. In fact, during an earthquake, the fault breaks, and the waves propagate toward the site at a speed close to the speed of the shear wave (Gheitarany *et al*., 2013) [12]. In the near field, the generated waves arrive at the site almost at the same time, which leads to the occurrence of a detectable velocity pulse in the earthquake. This important feature in near-field records is known as the directivity effect (Samami *et al*., 2024) [26]. Many studies have been done on engineering structures, and the results show it. The pulse of records in the near field is effective in the drift of the first floor and the maximum drift of the floors and increases the drift of the structure (Aghazadeh *et al*., 2019) [1].

And then the damage to the structure increases, especially when the period of the speed pulse is close to the period of the structure. Therefore, considering the effect of pulse in the analysis of seismic risk seems to be necessary (Gheitarani *et al*., 2024) [9]. A directional effect has not been seen in classical seismic risk analysis. Therefore, it is not suitable to estimate the seismic risk of the nearby area using classical seismic risk analysis (Zakerhaghighi *et al*., 2015) [30]. In recent years, efforts have been made to consider the impact of the near-field pulse in seismic risk analysis. The existence of a pulse in the earthquake record causes the range of ground motion to increase. Much research has been done to model the amplitude increase of the response spectrum due to the pulse effect. For this purpose, two different ways of thinking have been proposed, which are:

- Modeling with a uniform increase or decrease of the response spectrum in all periods.

- Increasing the amplitude of the response spectrum over a range of periods close to the pulse period.

Tutang *et al*. (2007) presented a framework for considering the directionality effect in PSHA. In this method, the amplitude of the response spectrum is increased in the range around the pulse period (the pulse period is chosen as the center) and no assumption has been made for the level of amplitude increase (Kahvand *et al*., 2015; Aydin *et al*., 2020) [13, 4]. Also, the period range is completely experimentally calibrated. Shahi and Baker (2011) modified the framework based on the pulse shape characteristics of the earthquake record. They detected the pulse in a direction different from the normal fault direction and used it to calibrate the pulse prediction model. Their revised framework includes a model for predicting the probability of pulse occurrence for the geometry of the seismic source site and pulse period distribution. Ciocarelli and Irolino (2012), by applying changes in the classical seismic risk analysis formulas, considered the directional effects in seismic risk analysis (Naghibi Iravani *et al*., 2024a) [24].

They considered the fault geometry in full and the distance vector in more detail. They also calculated the probability of pulse occurrence according to the geometrical conditions of the site, and by using the attenuation relation modified by Baker (2008), they included the pulse effect in the response spectrum. Compared to the previous methods, this method includes the effects of the near field in the analysis of seismic risk in a more comprehensive way. In this article, the basics of probabilistic seismic risk analysis in the near area are explained. By providing an example, the effects of a fault pulse on different sites have been investigated. Finally, the interpretation of the results of different methods of seismic risk analysis has been done.

2. Probabilistic seismic hazard analysis of the near NS-PSHA area

The main goal of probabilistic seismic risk analysis is to calculate the probability of exceeding a certain limit for all possible earthquakes. Cornell was the first to present a classical method for calculating (PSHA). Classical probabilistic seismic hazard analysis (Cornell's method) estimates the seismicity of the region by considering uniform distribution over the area and the large area (Aghazadeh *et al*., 2017; Aghazadeh *et al*., 2018) [2, 3]. To consider directional effects in seismic hazard analysis, the classic PSHA can be modified by highlighting the ground motion feature, which is referred to as line analysis.

$$\lambda_{sa} = \upsilon . \iint G_{(s_a|M,R)}(S_a|M,R).f_{M,R}(M,R).dM\,dR \tag{1}$$

In this relation, M is the magnitude of the earthquake, R is the distance from the site to the source of the earthquake, ν is the average annual rate of occurrence of the source earthquake, $f_{M,R}(M,R)$ The joint probability density function of magnitude and distance, and $G_{(s_s|M,R)}$ Past conditional probability S_a For a certain value, it is large and distance. To consider the pulse effect, the method presented by Ciocarelli and Irolino (2012) has been used (Khanian *et al*., 2019; Aghazadeh *et al*., 2019) [18, 1]. For this purpose, it is assumed that there are two faults in a specific place and in the nearby area, one of which produces a normal earthquake and the other is capable of producing a pulse earthquake record. So, NS-PSHA includes two risk expressions. In equation 2, an expression for the absence and one for the coincidence of the pulse, respectivelyand , $\lambda_{sa,Nopulse}$ another $\lambda_{sa,Pulse}$ is shown (Gheitarani *et al*., 2013; Aghazadeh *et al*., 2018) [11, 3].

$$\lambda_{sa} = \lambda_{sa,Nopulse} + \lambda_{sa,Pulse} \tag{2}$$

Since the effect of these two parameters depends on the probability of pulse occurrence, the weight of the two terms of relation (2) is determined by the probability of pulse occurrence. Therefore, in PSHA NS- three new and important issues should be considered: 1) probability of pulse occurrence, 2) pulse period, and 3) impact of pulse on the amplitude of ground motion. To calculate the probability of occurrence of the pulse, the stochastic model for predicting the probability of occurrence of the pulse, which was presented by Irolino and Cornell (2008), was used (GHADARJANI & GHEITARANI, 2013; Sarabi *et al*., 2023) [7, 21]. This model only depends on the geometric characteristics described in Fig 2 and it is different for the fault along the slip direction and the slip slope. Equations (3) and (4) express the probability of pulse occurrence for strike-slip fault and strike-slip fault, respectively (Karimimansoob *et al*., 2024-b) [16].

$$W_{Pulse} = P(Pulse|R,s,\theta) = \frac{e^{0.859-0.111R+0.019s-0.044\theta}}{1+e^{0.859-0.111R+0.019s-0.044\theta}} \tag{3}$$

$$W_{Pulse} = P(Pulse|R,d,\varphi) = \frac{e^{0.553-0.055R-0.027d-0.027\varphi}}{1+e^{0.553-0.055R-0.027d-0.027\varphi}} \tag{4}$$

In relations 3 and 4, S is the distance of the focal point from the site in the strike-slip fault and d is the focal distance from the site in the strike-slip fault, which is measured in the direction of failure. θ The angle between the fault and the path of the center of the focus to the site φ is the angle between the fault plane and the path that connects the center of the focus to the site, and R is the shortest distance between the location of the fracture and the site (Gheitarani *et al*., 2020; Maleki *et al*., 2024) [10, 19]. The range of changes of the variables of relationship 3 and 4 is shown in Table 1.

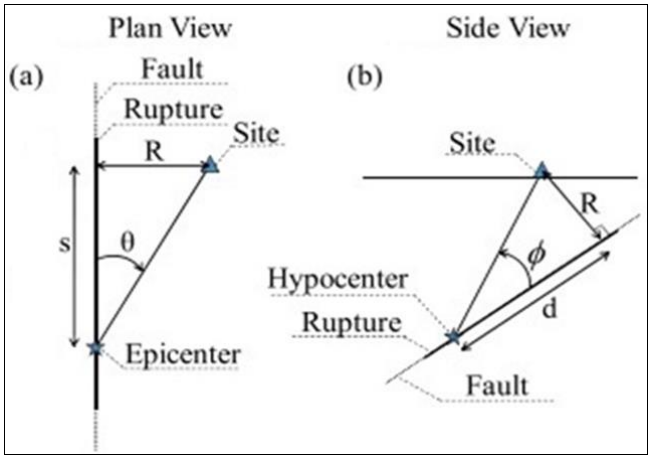

Source: Yaghmaei-Sabegh *et al*., 2017

Fig 1: Geometrical parameters (a) sliding direction (b) sliding slope

Table 1: The range of changes of the variables used in relation 3 and 4

	s (km)	d (km)	θ	φ	R(km)
Straight-slip fault	0-40	-	0-90	-	0-30
Slope-slip fault	-	0-20	-	0-90	5-30

Assuming the existence of two modes of pulse occurrence and non-occurrence, the probability of pulse non-occurrence is calculated using equation 5.

$$W_{Nopulse} = P(Nopulse) = 1 - P(Pulse) \quad (5)$$

As mentioned, apart from calculating the probability of pulse occurrence, the pulse period and the impact of the pulse on the range of ground motion should also be included in risk analysis calculations.
Somerville, 2003, has stated in his studies that the pulse period depends on the source parameters, including the time of sliding on the fault and the size of the fault, and generally increases with the magnitude of the earthquake (Aydin *et al*., 2020; Dizaji *et al*., 2023) [4, 5]. The value of the pulse period (Tp) depends on the magnitude of the earthquake. Our linear relationship between the magnitude of the torque and the logarithm of Tp has been confirmed by all those who have researched this issue. In this research, the relation of Ciocarelli and Irolino (2012) is used to predict the pulse period, which is presented in relation 6 (Aghazadeh *et al*., 2017) [2].

$$Ln(T_p) = -6.19 + 1.07M_w \quad (6)$$

To consider the pulse on the ground motion amplitude in NS-PSHA, modifications should be applied to the ground motion prediction equations (GMPE). To have a proper GMPE that includes the pulse effect, you can use Baker's model (2008). This model models the changes resulting from the pulse in the elastic spectrum of the normal record. Whose mathematical relationship is in the form of the following relationship (Ghadarjani *et al*., 2013).

$$\overline{Ln(S_a(T))} = Ln(S_a(T)) + e^{-(Ln(T/T_p))} \quad (7)$$

In this equation $Ln(S_a(T))$, the logarithm of the normalized GMPEs spectral acceleration and $\overline{Ln(S_a(T))}$ the logarithm of spectral acceleration of GMPEs has been modified. Equations 8 and 9 are obtained from the expansion of equation 2 for a fault whose failure mechanism is not yet defined.

Z is a vector that describes the distance between the earthquake source and the site.

$$\lambda_{S_a,nopulse} = \upsilon \iint W_{Nopulse} G_{(S_a|M,Z)}(S_a|M,Z).f_{M,Z}(M,Z).dM.dZ \quad (8)$$

$$\lambda_{S_a,pulse} = \upsilon \iiint W_{Pulse} G_{(S_a,\mathrm{mod}|M,Z,T_p)}(S_a|M,Z,T_p).f_{(T_p|M,Z)}(T_p|M,Z).f_{M,Z}(M,Z).dM.dZ.dT_p \quad (9)$$

Equation 8 is related to the pulse-free record and is weighted according to the probability of no pulse occurrence, and the rest of the terms are the same as Equation 1. Equation 9 is related to the record with a pulse, which is determined by the probability weight of the pulse (Sarabi & Norouzian, 2023) [21]. It is possible to calculate the spectrum of the record with a pulse, from

modifying the existing GMPEs, and with the index $G_{(S_a,\mathrm{mod}|M,Z,T_P)}$ has been investigated. Hence, the modification of conventional GMPEs depends on the pulse period after the distribution $f_{(T_P|M,Z)}(T_P|M,Z)$ required for analysis.

$f_{M,Z}(M,Z)$ The joint probability distribution between earthquake magnitude and geometric parameters is the same as the normal PSHA. The difference is in the more defined details between the source and the site according to the distance variables in relation 1 (Sarabi & Norouzian, 2023) [21].

To describe the Z vector, the type of failure must be determined first. For a unique landslide source with fixed dimensions and geographic location, the geometric characteristics required to calculate the seismic risk are:

The length of the fracture (which is less than or equal to the length of the fault), the position of the fracture on the fault P, and the location of the epicenter E are shown in Fig 1. These parameters are determined by existing relationships and R, S, θ vectors. Therefore, we replace vector Z with vectors E, P, and L in equations 8 and 9, and equations 10 and 11 are obtained.

$$\lambda_{S_a,nopulse} = \upsilon \iint\iint W_{Nopulse} G_{(S_a|M,L,P,E)}(S_a|M,L,P,E).f_{(P,E|M,L)}(P,E|M,L).f_{(L|M)}(L|M).f_M(M).dM.dL.dP.dE \quad (10)$$

$$\lambda_{S_a pulse} = \upsilon \iiint\iint W_{pulse} G_{(S_{a,MOD}|M,L,P,E,T_P)}(S_{a,MOD}|M,L,P,E,T_p).f_{(T_P|M)}(T_P|M).f_{(P,E|M,L)}(P,E|M,L).f_{(L|M)}(L|M).f_M(M).dM.dL.dP.dE.dT_P \quad (11)$$

The numerical solution of equations 10 and 11 is like the flowchart shown in Fig 2.

3. Model and results

To investigate the effects of the pulse in the near area of a fault, a hypothetical 200 km long slip has been defined with four sites.

The results of NS-PSHA are compared with the results of conventional and deterministic probabilistic risk analysis. Hypothetical sites are in line with the fault and are located at a distance of 5, 10, 15, and 20 km from the highest point of the fault. The location of the site relative to the fault is shown in Fig 3. For the seismic characteristics of the region, the b value (Gutenberg-Richter constant) is assumed to be equal to one, and the maximum and minimum values are assumed to be equal to 7.5 and 4.5, respectively.

Also, to reduce the calculations, the large distribution with three discrete values 5, 6, and 7 is considered. The discrete probability is calculated according to the magnitude of the earthquake according to the type of probability density function model (Gutenberg-Richter or characteristic earthquake). Selected seismic intensity (IM), and elastic spectral acceleration for the return period of 10,000 years are considered. To calculate the elastic spectral acceleration, four reduction relations of NGA08, Abrahamson and Silva (2008), Burr Watkinson (2008), Campbell and Bozorgnia (2008), and Chiu Viang (2008) have been used.

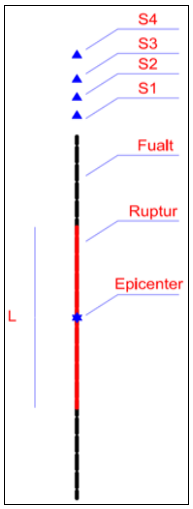

Fig 2: Geometric characteristics of the fault and the studied site

In the site, the spectrum obtained from PSHA is lower than all the spectra obtained from other methods. In fact, in the near field area, the PSHA method underestimates the risk. The spectrum obtained from the NS-PSHA method shows the pulse effects caused by near-field waves. The pulse caused by the directional effect affects the acceleration spectrum in the range of 0.1 to 2 seconds, and the biggest difference between this spectrum from the PSHA spectrum is in 0.5 seconds (Dizaji *et al*., 2023) [5].

On the site, you can also see the impact of the pulse on the acceleration spectrum. In this limited site, the influence in different periods and the increase of the range of the spectrum has been reduced compared to the site (Zaker Haghighi *et al*., 2014) [29]. This trend of reduction in the site is evident so that the increase of the range of the spectrum in the period is 0.1 to 1. This downward trend continues on the site as well, so that the difference between the two spectra reaches zero. In all sites, the

DSHA method has estimated the amount of risk more than the other two methods, and with increasing distance, the value of the acceleration spectrum in this method decreases.

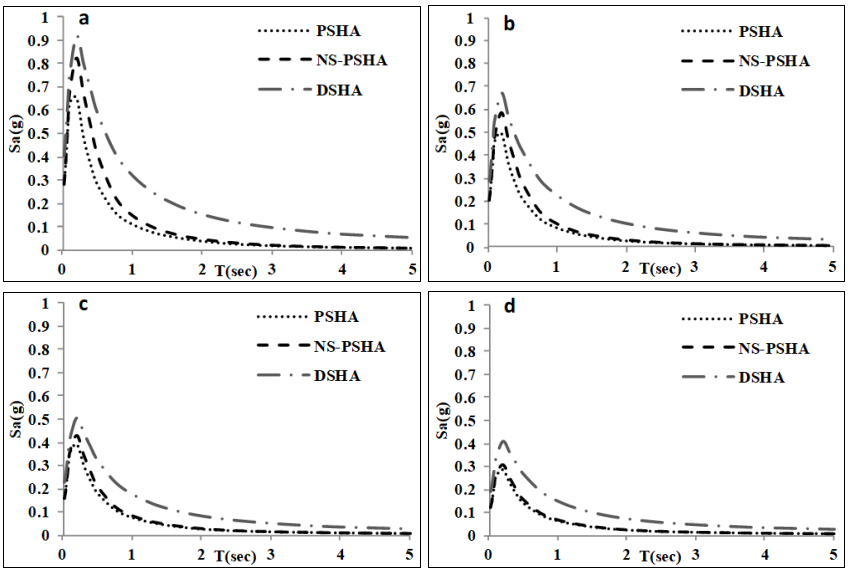

Fig 3: Acceleration spectra obtained from the methods PSHA (dashed line), NS-PSHA (black dashed line), DSHA (gray line and dot) a) site b) site c) site d) site

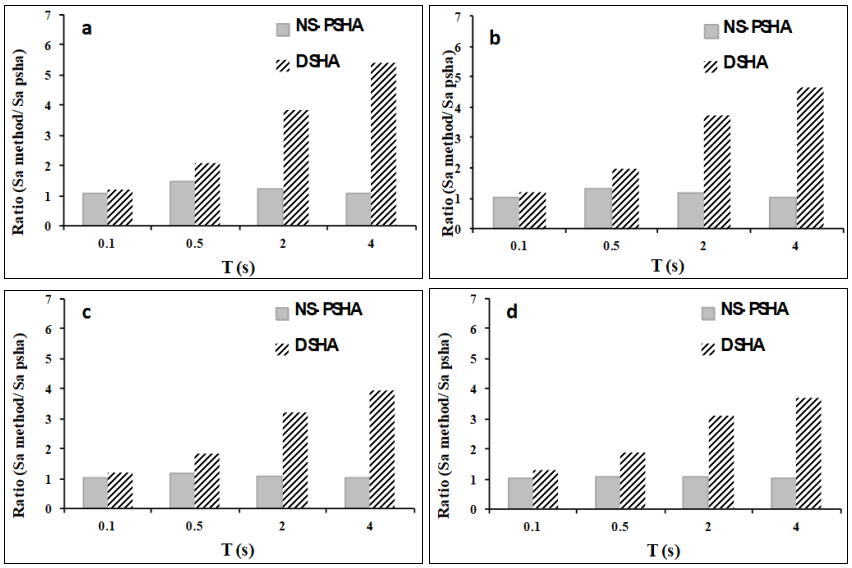

Fig 4: Ratio of spectral acceleration resulting from NS-PSHA (gray column), DSHA (dashed line column) methods to PSHA a) site b) site c) site d) site

Fig 4 shows the ratios of the spectral acceleration of different methods to the spectral acceleration of PSHA. The maximum ratio for NS-PSHA and DSHA methods is equal to 1.46, and 5.48 respectively. In the NS-PSHA method, the maximum ratio has occurred around the period of 0.5 seconds, while in the DSHA method, it has occurred in the above periods. It can be seen that the spectral acceleration ratio of the DSHA method is very different from other methods in the period of periods higher than one second (Khanian *et al*., 2013; Mohammad & Norouzian, 2023) [17, 20].

The reason for this can be explained in the following way: Firstly, the investigated index is the ratio of spectral acceleration obtained from different methods compared to PSHA, and in sites where a fault is considered, the amount of spectral acceleration obtained from PSHA is much higher than DSHA is less. With the increase in the number of faults, the amount of spectral acceleration resulting from the PSHA method has increased, while the acceleration value obtained from the DSHA method may remain constant. Secondly, larger magnitudes affect the spectral acceleration in high periods, so the spectrum resulting from DSHA in high periods is very different from the spectrum of PSHA. In Fig 5, you can also see the effect of the pulse at different distances. The maximum ratio of NS-PSHA spectrum in the site is equal to 1.32, 1.18, and 1 respectively, all of which occurred within 0.5 seconds.

4. Conclusion

In this research, taking into account the important characteristics of earthquakes in the near area in risk analysis, the details of the NS-PSHA method were presented. Risk analysis calculations were done by selecting a 200 km long fault for four sites located at a distance of 5, 10, 15, and 20 km from it. The sites have been selected in such a way that the probability of pulse

occurrence is high. For the target site, seismic risk analysis for three different risk analysis methods was compared for a return period of 10,000 years. The obtained results indicate that the pulse effects have a significant impact on the acceleration spectrum in close distances so that in some periods this difference reaches 50%. As the distance increases, the impact of the pulse decreases. In addition, it was shown that the DSHA method is very different from the PSHA in high periods, but the NS-PSHA method in high periods does not have a great effect on increasing the range of the spectrum.

5. References

1. Aghazadeh M, Karimzadeh I, Ganjali MR. Dextran grafted nickel-doped superparamagnetic iron oxide nanoparticles: Electrochemical synthesis and characterization. Journal of Nanostructures. 2019; 9(3):531-538.
2. Aghazadeh M, Karimzadeh I, Ganjali MR, Malekinezhad A. Al3+ doped Fe3O4 nanoparticles: A novel preparation method, structural, magnetic and electrochemical characterizations. International Journal of Electrochemical Science. 2017; 12(9):8033-8044.
3. Aghazadeh M, Karimzadeh I, Ganjali MR, Maragheh MG. Electrochemical fabrication of praseodymium cations doped iron oxide nanoparticles with enhanced charge storage and magnetic capabilities. Journal of Materials Science: Materials in Electronics. 2018; 29:5163-5172.
4. Aydin AC, Yaman Z, Ağcakoca E, Kiliç M, Maali M, Aghazadeh Dizaji A. CFRP effect on the buckling behavior of dented cylindrical shells. International Journal of Steel Structures. 2020; 20:425-435.
5. Dizaji AA, Kiliç M, Maali M, Aydin AC. Buckling behaviour of dented short cylindrical shells retrofitted with CFRP. Proceedings of the Institution of Civil Engineers-Structures and Buildings. 2023; 176(1):62-75.
6. Farrokhirad E, Gheitarani N. How Green Wall Imploratory Strategies Can be Facilitated and Optimized through Public Engagement? European Online Journal of Natural and Social Sciences. 2024; 13(2):128.
7. Ghadarjani R, Gheitarani N. Methods for enhancing public participation in the rehabilitation and renovation of deteriorated housing case study: Joulan neighborhood in the Hamedan City, 2013.
8. Ghadarjani R, Gheitarani N, Khanian M. Examination of city governorship pattern and citizen participation as a new approach to city management in region 5 of Isfahan municipality using T-test in SPSS. European Online Journal of Natural and Social Sciences. 2013; 2(4):601.
9. Gheitarani N, Arash Sohrabi S, Naghibi Iravani S, Dehghan S. Analyzing the Mechanism of the Possible Effect of Place Attachment of Residents of Iranian Neighborhoods in Improving the Level of Quality of Life (Study Example: Joolan Neighborhood in Hamedan City). European Online Journal of Natural and Social Sciences. 2024; 13(1):42.
10. Gheitarani N, El-Sayed S, Cloutier S, Budruk M, Gibbons L, Khanian M. Investigating the mechanism of place and community impact on quality of life of rural-urban migrants. International Journal of Community Well-Being. 2020; 3:21-38.
11. Gheitarani N, Ghadarjani R, Kahvand M, Mehrabadi SAM. Explaining the effective measures in decreasing the vulnerability of urban area against earthquake using AHP model (case study: Tehran, a metropolis). Journal of Basic and Applied Scientific Research. 2013; 3(8):675-681.
12. Gheitarany N, Mosalsal A, Rahmani A, Khanian M, Mokhtari M. The role of contemporary urban designs in the conflict between vehicle users and pedestrians in Iran cities (case study: Hamedan City). World Applied Sciences Journal. 2013; 21(10):1546-1551.
13. Kahvand M, Gheitarani N, Khanian MOJTABA, Ghadarjani RAZIEH. Urban solid waste landfill selection by SDSS. Case study: Hamadan. Environment Protection Engineering. 2015; 41(2):47-56.
14. Karimimansoob V, Mahdaviparsa A, Sadigh Sarabi M, Safaei-Mehr M. Application of BIM in Energy Conservation in Low-Cost Housing in Case of Study in Dallas Independent School Residential District, Texas. European Online Journal of Natural and Social Sciences. 2024; 13(3):188.a
15. Karimimansoob V, Mahdaviparsa A, Sadigh Sarabi M, Safaei-Mehr M. Application of BIM in Energy Conservation in Low-Cost Housing in Case of Study in Dallas Independent School Residential District, Texas. European Online Journal of Natural and Social Sciences. 2024; 13(3):188.
16. Karimimansoob V, Safaei-Mehr MM, Norouzian M, Gheitarani N. Scrutinizing of City Taxes Effects on Final Housing Price in Hamedan. European Online Journal of Natural and Social Sciences. 2024; 13(3):235.b
17. Khanian M, Bolouhar B, Gheitarany N, Nezhad SM. Studying the causes of vitality in traditional markets of Iran (Case Study: Shoemaking Order of Central Market of Hamadan). World Applied Sciences Journal. 2013; 22(6):831-835.
18. Khanian M, Serpoush B, Gheitarani N. Balance between place attachment and migration based on subjective adaptive capacity in response to climate change: The case of Famenin County in Western Iran. Climate and Development. 2019; 11(1):69-82.
19. Maleki M, Gheitaran N, El-Sayed S, Cloutier S, Gaelle Giraud E. The development and application of a localised metric for estimating daylighting potential in floor plate. International Journal of Ambient Energy. 2024; 45(1):2277310.
20. Norouzian MM, Sarabi MS. Analyzing the dynamic data of Mashhad metro line 1 tunnel using seismic table. ISAR Journal of Science and Technology. 2023; 1(2):1-9.
21. Sarabi MS, Norouzian MM, Karimimansoob V. Analyzing and investigating the effects of Naqadeh earthquake aftershocks in West Azerbaijan on the results of probabilistic seismic risk estimation using clustering analysis. ISAR Journal of Science and Technology. 2023; 1(1):38-45.
22. Mohammad MSS, Mehdi Norouzian. Analyzing the dynamic data of Mashhad metro line 1 tunnel using seismic table. ISAR Journal of Science and Technology. 2023; 1(1):1-9.

23. Naghibi Iravani S, Arash Sohrabi S, Gheitarani N, Dehghan S. Spatial Configuration as a Method to Measure the Actual and Potential Ability of Spaces Used by Indoor and Outdoor Users. European Online Journal of Natural and Social Sciences. 2024b; 13(2):90.
24. Naghibi Iravani S, Karimimansoob V, Arash Sohrabi S, Gheitarani N, Dehghan S. Applying Fuzzy Logic and Analysis Hierarchy Process (AHP) in the Design of Residential Spaces; Case of Study: Arak City. European Online Journal of Natural and Social Sciences. 2024a; 13(2):144.
25. Naghibi Iravani S, Sohrabi SA, Gheitarani N, Dehghan S. Providing a Pattern and Planning Method for Footpaths and Sidewalks to Protect Deteriorated and Vulnerable Urban Contexts. European Online Journal of Natural and Social Sciences. 2024; 13(1):1.b
26. Samami H, Naghibi Iravani S, Arash Sohrabi S, Gheitarani N, Dehghan S. Evaluation and Optimization of Building Greening Methods in Four Different Climates Using Building Information Modeling (BIM). European Online Journal of Natural and Social Sciences. 2024; 13(1):27.
27. Mohammad Sadigh Sarabi VK, Mohammad Mehdi Norouzian. Analyzing and investigating the effects of Naqadeh earthquake aftershocks in West Azerbaijan on the results of probabilistic seismic risk estimation using clustering analysis. ISAR Journal of Science and Technology. 2023; 1(1):38-45.
28. Yaghmaei-Sabegh S, Ebrahimi-Aghabagher M. Near-field probabilistic seismic hazard analysis with characteristic earthquake effects. Natural hazards. 2017; 87:1607-1633.
29. Zaker Haghighi K, Gheitarani N, Khanian M, Taghadosi R. Examination of effects of urban street configuration on the amount of commercial buildings establishment (according to natural movement theory), Case study: Hamedan. European Online Journal of Natural and Social Sciences. 2014; 3(1):20.
30. Zakerhaghighi K, Khanian M, Gheitarani N. Subjective quality of life; assessment of residents of informal settlements in Iran (a case study of Hesar Imam Khomeini, Hamedan). Applied research in quality of life. 2015; 10:419.